

Generating Euler Diagrams Through Combinatorial Optimization

Peter Rottmann¹ , Peter Rodgers² , Xinyuan Yan³ , Daniel Archambault⁴ , Bei Wang³ , Jan-Henrik Haunert¹ 

¹University of Bonn, Institute of Geodesy and Geoinformation, Germany

²University of Kent, UK

³University of Utah, USA

⁴Newcastle University, UK

Abstract

Can a given set system be drawn as an Euler diagram? We present the first method that correctly decides this question for arbitrary set systems if the Euler diagram is required to represent each set with a single connected region. If the answer is yes, our method constructs an Euler diagram. If the answer is no, our method yields an Euler diagram for a simplified version of the set system, where a minimum number of set elements have been removed. Further, we integrate known wellformedness criteria for Euler diagrams as additional optimization objectives into our method. Our focus lies on the computation of a planar graph that is embedded in the plane to serve as the dual graph of the Euler diagram. Since even a basic version of this problem is known to be NP-hard, we choose an approach based on integer linear programming (ILP), which allows us to compute optimal solutions with existing mathematical solvers. For this, we draw upon previous research on computing planar supports of hypergraphs and adapt existing ILP building blocks for contiguity-constrained spatial unit allocation and the maximum planar subgraph problem. To generate Euler diagrams for large set systems, where the proposed simplification through element removal becomes indispensable, we also present an efficient heuristic. We report on experiments with data from MovieDB and Twitter. Over all examples, including 850 non-trivial instances, our exact optimization method failed only for one set system to find a solution without removing a set element. However, with the removal of only few set elements, the Euler diagrams can be substantially improved with respect to our wellformedness criteria.

CCS Concepts

• **Human-centered computing** → **Information visualization**; • **Theory of computation** → **Integer programming**; • **Mathematics of computing** → **Hypergraphs**;

1. Introduction

Euler diagrams are frequently used to visualize set systems. They represent each set as a region in the plane that is bounded by a closed curve. An area in an Euler diagram that is occupied by one or multiple regions indicates the existence of set elements that are contained in the corresponding sets and in no other set. An advantage of Euler diagrams is that they are intuitive to understand. However, they can become cluttered even for medium-sized set systems. For a given set system, it is possible that no Euler diagram exists when requiring the regions to be connected. Previous approaches [RZF08, SA08] split sets into two or more separate regions. However, splitting makes it harder to identify regions belonging to the same set, and increases the overall number of regions in the visualization.

Our work addresses two research problems. First, none of the existing methods can decide for a given set system whether an Euler diagram with a single connected region for each set exists, let alone generate an Euler diagram in every case where it is possible. Second, Euler diagrams have typically been considered as a

tool to visualize set systems without loss of information. We think Euler diagrams can be used as a tool to visually summarize large set systems, but for this the generation of Euler diagrams has to be combined with a simplification of the given data.

Our contribution is a new combinatorial optimization approach. Given a set system as input, our goal is to compute a simplified but still similar version of it that can be drawn nicely as an Euler diagram. The simplification is achieved by removing some set elements from the set system. To quantify the loss of information caused by the removal of elements, we assume that every element has a weight expressing the cost of its removal. For example, the weight of each element may be one, or it can be equal to the number of sets containing the element. More generally, any measure expressing the importance of the element can be applied.

Our most important contribution is an exact optimization method that minimizes the total weight of the removed set elements while ensuring that the resulting simplified set system can be embedded in the plane as an Euler diagram with a single connected region for each set. Moreover, we contribute multiple extensions of our

method to integrate additional optimization criteria that improve the resulting Euler diagram with respect to known wellformedness conditions [RZP11]. For large problem instances, we introduce an efficient heuristic method. We conduct experiments with both the exact method and the heuristic on realistic problem instances and assess the quality of their solutions as well as their efficiency.

2. Preliminaries and basic problem

To discuss our contribution in the context of related work and develop our methods, we view the given set system as a *hypergraph*. A hypergraph $H = (V, E)$ consists of two sets, a vertex set V and a hyperedge set E , where each hyperedge $X \in E$ is a subset of V , i.e., $X \subseteq V$. In the hypergraph representation of a set system, every vertex in V corresponds to a set element and every hyperedge in E to a set. A *support* of a hypergraph $H = (V, E)$ is a graph G with vertex set V such that each vertex set $X \in E$ (i.e., each hyperedge) *induces* a connected subgraph in G , meaning that the subgraph of G whose node set is X and whose edge set contains an edge for every two nodes in X that are adjacent in G is connected. In the context of Euler diagrams, it is most interesting to find a *planar support* of a given hypergraph H , i.e., a support of H that can be drawn in the plane without edge crossings; see Fig. 1. In essence, a planar support of a given hypergraph can serve as the dual graph of the Euler diagram that is to be constructed; see Figs. 2 and 3.

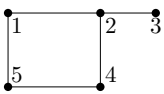


Figure 1: A planar support of the hypergraph with nodes $1, \dots, 5$ and hyperedges $\{1, 2, 3\}$, $\{1, 4, 5\}$, $\{2, 4\}$, each inducing a connected subgraph.

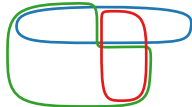


Figure 2: An Euler diagram whose dual graph is the planar support in Fig. 1. The three regions correspond to the three hyperedges of the hypergraph.

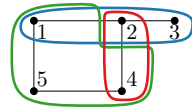


Figure 3: The planar support of the hypergraph in Fig. 1 superimposed with an Euler diagram using the planar support as its dual graph.

When we say that we remove an element v from a hypergraph $H = (V, E)$ we imply that v is removed from the vertex set V of H as well as from every hyperedge $X \in E$ in which v occurs. We introduce for every node $v \in V$ a weight $w(v) \in \mathbb{R}_{>0}$ measuring the cost of its removal. If the aim is to minimize the number of element removals, we set $w(v) = 1$ for each set element. Else, if the aim is to minimize the loss of set memberships, we set $w(v) = |\ell(v)|$, where $\ell(v)$ is the set of hyperedges containing v , i.e., $\ell(v) = \{X \in E \mid v \in X\}$. With $H - S$ we refer to the hypergraph resulting from a hypergraph $H = (V, E)$ after removing a set $S \subseteq V$ from it. With this, we are ready to state a basic problem that asks for an optimal simplification of a set system to generate an Euler diagram.

Problem 1 (SetSystemSimplification)

Given a hypergraph $H = (V, E)$ and a weighting $w: V \rightarrow \mathbb{R}_{>0}$, find a minimum-weight set $S \subseteq V$ such that $H - S$ has a planar support and return such a planar support as output.

We would like to point out that SetSystemSimplification has a solution with $S = \emptyset$ if and only if the given hypergraph H has a planar

support. Therefore, any exact optimization algorithm for SetSystemSimplification can be used as a tool to decide whether a hypergraph has a planar support. Since deciding whether a hypergraph has a planar support is NP-hard [JP87], we can conclude that SetSystemSimplification is NP-hard, too.

As our problem is NP-hard, there is no reasonable hope for an efficient exact algorithm. Therefore, we focus on an approach based on integer linear programming, which is a general method for solving combinatorial optimization problems and has the advantage that we can employ existing mathematical solvers. With this we can solve both the new problem SetSystemSimplification and the known problem of finding a planar support for a given hypergraph.

Solving SetSystemSimplification is insufficient as it neglects important criteria. Therefore, we will extend it to a multi-criterial problem, MCSetSystemSimplification, after reviewing wellformedness conditions for Euler diagrams. Both our exact method and our heuristic can deal with this extended problem.

3. Workflow

While we consider the exact optimization method and the heuristic for MCSetSystemSimplification as our main contribution, we also provide a complete workflow that yields an Euler diagram visualizing a simplified version of a given hypergraph. This workflow is illustrated in Fig. 4 for an artificial example and outlined below.

In Step 1 of our workflow, we replace every set of nodes that are contained in exactly the same hyperedges with a single node, yielding the *condensed hypergraph*. The motivation for this step is that nodes contained in exactly the same hyperedges should not be separated in the final visualization. Moreover, working with the condensed graph greatly reduces the running time of our methods. It is important to note, however, that this step may affect the existence of a planar support [vBKK*22]. Therefore, we may optionally skip this step, for example, if the aim is to compute a planar support of the original hypergraph.

In Step 2 of the workflow, the condensed hypergraph is used to compute the *superdual graph*, whose node set contains every node of the condensed hypergraph as well as a special node v_0 representing the outer face, and whose edge set contains every edge that may be useful for the dual graph of the Euler diagram. Next, in Step 3, a solution to MCSetSystemSimplification is computed in the form of a selection of nodes and edges of the superdual graph, which determines both the simplified hypergraph and the dual graph of the Euler diagram. This is achieved either with our exact optimization approach via integer linear programming or our heuristic method.

We use existing methods for the last three steps of our workflow. First, in Step 4, we compute a planar embedding of the dual graph generated in Step 3 [CP95]. In Step 5, the planar embedding is used to construct an initial Euler diagram [RZF08] that is guaranteed to contain only simple curves. Finally, in Step 6, the curves of the initial Euler diagram are smoothed [SAS16].

4. Related work

The visualization of set systems has been an active research topic for several years. A comprehensive study and classifica-

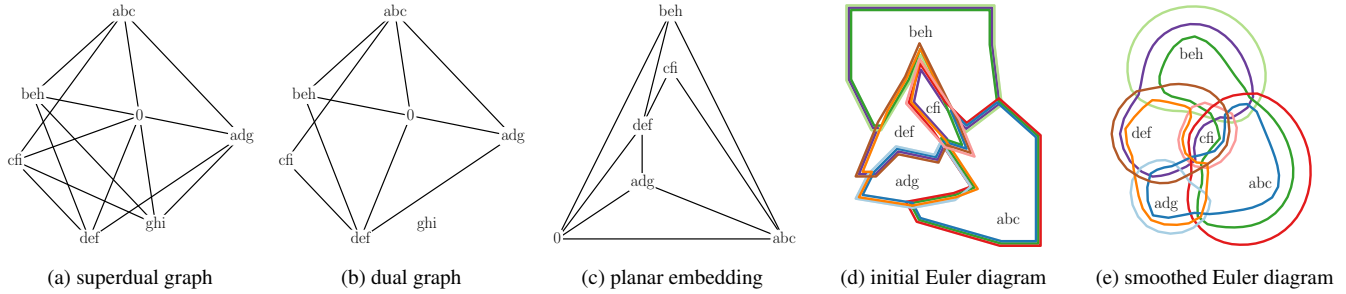


Figure 4: Results after different steps of our hypergraph visualization workflow. The input to the shown example is a set system consisting of nine sets, i.e., hyperedges: $a: \{1, 4, 7\}$, $b: \{1, 5, 7\}$, $c: \{1, 6, 7\}$, $d: \{2, 4\}$, $e: \{2, 5\}$, $f: \{2, 6\}$, $g: \{3, 4\}$, $h: \{3, 5\}$, $i: \{3, 6\}$. The set elements 1 and 7 are replaced by a single set element in the first step because both are contained by the same hyperedges. The label of each node refers to the sets containing it. The additional node labelled 0 represents the outer face. The results of Steps 2–6 are visualized by Figs. (a)–(e). For each set there exists one edge in the superdual graph that has to be selected to ensure the set’s connectivity if all set elements are selected. Since these edges constitute the non-planar graph $K_{3,3}$, a node of the superdual graph has to be removed to generate a planar dual graph.

tion of the literature into six categories was done by Alsallakh et al. [AMA*16]. Here, we focus on Euler diagrams, which have been investigated by two overlapping communities: information visualization and graph drawing.

4.1. Euler diagrams

Much research on Euler diagrams has focused on the definition of *wellformedness conditions* and how to ensure them. These conditions describe properties of Euler diagrams which target an improved comprehension of the diagrams. Sets are represented by labelled closed curves and set intersections are represented by zones, which are regions enclosed by the required closed curves. Typical wellformedness conditions include:

- **Connected zones:** each zone in the diagram is connected, broken in Fig. 5a.
- **No concurrency:** no pair of curves run concurrently, broken in Fig. 5b.
- **Transversality:** intersecting curves always intersect transversally (that is they cross, rather than just ‘touch’), broken in Fig. 5c.
- **Simplicity:** all curves are simple curves. A curve is simple if it does not cross itself, broken in Fig. 5d.
- **No triple points:** there are no triple points of intersection among the curves, broken in Fig. 5e.
- **Unique curve labels:** no curve label is used more than once, broken in Fig. 5f.

For a more formal definition of wellformedness conditions, see [SRHT07]. To verify the importance of each property, Rodgers et al. [RZP11] conducted a user study measuring time and errors during the completion of given tasks. Disconnected zones and concurrent curves caused significant errors and increase in completion time. Moreover, representing a set with more than a single curve had a significantly adverse impact on task completion time.

Early approaches to Euler diagram embedding aimed to create wellformed Euler diagrams with rather strict conditions. Flower and Howse [FH02] defined *concrete Euler diagrams*, which did not break any of the wellformedness conditions above. However,

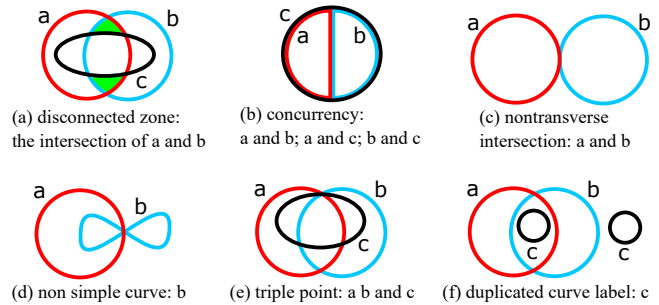


Figure 5: Examples of wellformedness conditions.

strictly requiring all of these conditions, means many set systems cannot be drawn.

Methods for generating Euler diagrams with relaxed wellformed conditions have been developed by Rodgers et al. [RZF08] and Simonetto and Auber [SA08]. However, these allow concurrency and duplicated curve labels. Moreover, these methods are heuristic and may introduce duplicated curve labels even when it is unnecessary. Since some of the existing methods (e.g., [SAA09]) yield Euler diagrams that can look distorted and stretched, EulerSmooth has been developed to smooth the curves of an existing Euler diagram [SAS16]. For achieving this goal, the algorithm applies a curve shortening flow approach. During this approach, the algorithm ensures that every set element stays within the correct zone using a force-directed edge-aware algorithm, ImPrEd [SAAB11]. SPEULER constructs Euler diagrams where set elements are arranged using circular layouts [KGWD22]. The resulting Euler diagrams are wellformed, which is partly a result by only allowing neighboring zones with no concurrency. RectEuler represents set-like data as Euler diagrams using rectangles as enclosing curves [PKS*23]. The resulting Euler diagrams are wellformed. However, they split the diagram into multiple diagrams if necessary. Additionally, there exist approaches for drawing the set elements of set systems as glyphs within the corresponding region of the Euler diagram [Bra12].

Recently, Zhou et al. [ZRPW23] presented a method for the simplification of hypergraphs and used Euler-like diagrams to visualize the results, but the simplification method does not consider criteria regarding the resulting visualization. Oliver et al. [OZZ23] presented a method for hypergraph simplification and visualization which, however, does not use Euler diagrams. Instead, the hyperedges are represented as polygons, whose vertices are the nodes.

4.2. Hypergraph drawings and planar supports

In the graph drawing community, a set system is usually viewed as a hypergraph, and different types of hypergraph drawings are considered. Mäkinen [Mäk90] introduced two types of drawings, which are called *edge standard* and *subset standard*. The latter type includes *vertex-based Venn diagrams*, which were defined by Pollock [JP87] and which correspond to the type of Euler diagrams that we address with our work, i.e., Euler diagrams that are based on planar supports. Later, vertex-based Venn diagrams were generalized into *subdivision drawings* [KvKS09]. Johnson and Pollock [JP87] also showed that it is NP-hard to decide whether a given hypergraph has a planar support. Moreover, they presented an efficient algorithm that yields a *tree support* if it exists, i.e., a planar support that is a tree. Following up on this, efficient algorithms were developed that can deal with edge weights to express preferences for including certain edges in a tree support [KS03, KMN14]. Also, it is known that one can efficiently decide whether a hypergraph has a planar support that is a path [KS03] or a *path-based tree support* [BKM*11], i.e., a planar support that is a tree such that every hyperedge induces a connected path in it.

Another line of research has dealt with finding planar supports for hypergraphs with special properties. Brandes et al. [BCPS11] presented an efficient algorithm for hypergraphs that are closed under intersections and differences, i.e., every intersection and difference of two hyperedges is also a hyperedge. Moreover, it is known that a hypergraph has a planar support if there is a non-empty intersection of all hyperedges [CR05], there are at most eight hyperedges [VV04], or the hypergraph results from the intersection of two families of regions that have a special property, called non-piercing [RR18]. None of the existing methods, however, can decide for an arbitrary hypergraph whether it has a planar support.

Recently, van Bevern et al. [vBKK*22] studied the role of twins in computing planar supports, where two vertices are twins if they occur in exactly the same hyperedges. They showed that when replacing a set of twins by a single vertex, the hypergraph may cease to have a planar support. However, the proof by Johnson and Pollock [JP87] shows that even for hypergraphs without twins it is NP-hard to decide whether a planar support exists. Our method for computing a planar support can deal with hypergraphs that contain twins, but we propose an optional pre-processing step to replace each set of twins by a single node to ensure that it will be represented as a single connected zone in the output Euler diagram.

4.3. Set visualizations

Several methods for set visualization have been developed that are related to hypergraph drawings or Euler diagrams.

LineSets aims at the reduction of clutter in representations of

set systems [ARRC11]. They represent each set of the system as a single continuous curve connecting all set elements. Similar to LineSets, Kelp Diagrams connects every zone corresponding to the same set with a line [DvKSW12]. If two sets share the same line, they are stacked and the lower one has an increased width. Additionally, the lines contain only straight segments. KelpFusion is an extension to Kelp diagrams [MRS*13]. It fills regions which are enclosed by lines corresponding to the same set.

A different approach of set visualization is UpSet [LGS*14]. UpSet is based on a matrix visualization where sets are represented in columns and set interactions are displayed in rows. MapSets draw a region containing the elements of a set [EHKP15]. However, these elements belong only to a single set, e.g. political parties. This results in no shared regions between sets. Additionally, the geometric position of set elements is fixed. As a result, the visualization is a partition of the plane containing set elements. ClusterSets are a generalization to MapSets which also allows single edges between points of the same set [GCH*21] and sets to be split into multiple regions. Similar, GMAP draws general graphs as geographic-like maps [GHK09]. The positions of the individual set elements are determined by the relation to adjacent set elements.

4.4. Integer linear programming

Integer linear programming is a general method for solving combinatorial optimization problems [NW88]. The approach is to encode a problem in the form of a set of variables, an objective function, and a set of constraints that have the form of an integer linear program (ILP), and to let a solver compute a variable assignment that is optimal under the constraints. The variable vector \mathbf{x} of an ILP contains integer variables. The objective function and the constraints of an ILP in canonical form are $f(\mathbf{x}) = \mathbf{c}^T \mathbf{x}$ and $A\mathbf{x} \leq \mathbf{b}$, $\mathbf{x} \geq 0$, respectively, where \mathbf{c} , A , and \mathbf{b} are given as constants. An equality constraint can be encoded in this form using two inequality constraints, and a binary variable can be expressed as an integer variable with upper bound 1. Although solving ILPs requires exponential time in the worst case, there exist ILP solvers that often perform well in practice. Especially for NP-hard problems, such as SetSystemSimplification, this approach is justifiable and often successful.

In the field of information visualization, there are two ILP-based methods that are most related to our own. Castermans et al. [TvGW*19] considered the problem of finding a support of a hypergraph with fixed vertex positions. The support is required to be a crossing-free straight-line graph, hence a stricter requirement than planarity is enforced. This can easily be achieved by forbidding the selection of crossing pairs of candidate edges. Our situation, however, is much more involved, since we need to ensure the planarity of the support without knowing the positions of its nodes. Another ILP-based method, MosaicSets, embeds a set system into a prescribed host graph, e.g., a regular grid [RWB*23]. There, the planarity is automatically ensured by choosing a planar host.

When modelling SetSystemSimplification as an ILP, the challenge lies in expressing constraints to ensure the connectivity requirement for hyperedges and the planarity requirement. For this, we adapt a formulation by Shirabe [Shi05] that enforces the connectivity of a region that results from the allocation of a set of faces

of a planar subdivision. Our constraint formulation for planarity is adapted from Chimani et al. [CHW19], who developed an ILP for the maximum planar subgraph problem, which for a given graph asks for a planar subgraph with the maximum number of edges.

5. Extended problem

In this section we extend SetSystemSimplification to model the most important wellformedness conditions, drawing upon the user study by Rodgers et al. [RZP11]. We require the connected zones wellformedness condition and consider the no-concurrency wellformedness condition in the objective function. We consider the unique curves labels wellformedness condition in the sense that we require that each set is represented as a connected region. However, we allow regions with holes. During the rendering process, we ensure that the Euler diagram satisfies the simplicity wellformedness condition by constructing the initial Euler diagram using a method that guarantees simple curves [RZF08]. The method that we apply for smoothing the Euler diagram [SAS16] considers the transversality wellformedness condition, but it does not strictly guarantee it. Before giving a formal definition of the extended problem, MCSetSystemSimplification, we provide technical details on how the input for the problem evolves from Steps 1 and 2 of our workflow.

In Step 1, which is optional, we compute for a given node-weighted hypergraph $H^* = (V^*, E^*)$ the condensed hypergraph $H = (V, E)$ and its node weighting w . We partition V^* into clusters, such that two nodes $u, v \in V^*$ are in the same cluster if and only if $\ell(u) = \ell(v)$, meaning that u and v are contained in exactly the same set of hyperedges. Then, for each cluster, we introduce a corresponding node in V , whose weight $w(v)$ we set to the total weight of the cluster. For every hyperedge $e^* \in E^*$, we add a corresponding hyperedge $e \in E$, which for each node in e^* contains the node representing its cluster. If we wish to skip Step 1, we simply set $H = H^*$. Only with Step 1, however, we ensure that our results fulfill the connected zones wellformedness condition.

In Step 2, based on $H = (V, E)$, we compute the superdual graph $G = (Z, F)$, from which we will select a subgraph that will serve as the dual graph of the Euler diagram. The node set of G is $Z = V \cup \{v_0\}$, where v_0 is a special node representing the outer face of the Euler diagram. The edge set F of G contains two types of edges, i.e., $F = F_1 \cup F_2$, where F_1 and F_2 are defined as follows:

- The set F_1 contains all edges that may be useful for a planar support of H , that is,

$$F_1 = \{\{u, v\} \mid u, v \in V, u \neq v, \ell(u) \cap \ell(v) \neq \emptyset\}. \quad (1)$$

This means that F_1 contains an edge for every two distinct nodes of H that are contained together in at least one hyperedge.

- The set F_2 contains edges that represent possible adjacency relationships between the outer face v_0 and the nodes in V . In principle, one could include one edge $\{v_0, v\}$ for each node $v \in V$. It is sufficient, however, to include only those edges whose selection has an influence on the objective function. We will introduce an objective function that rewards adjacency relationships between v_0 and nodes that are contained in few hyperedges (ideally, in only one hyperedge). Hence, we define

$$F_2 = \{\{v_0, u\} \mid u \in V, |\ell(u)| = \min_{w \in V} \{|\ell(w)|\}\}. \quad (2)$$

Selecting an edge $\{u, v\} \in F_1$ for the dual graph causes a violation of the no-concurrency wellformedness condition if the labels $\ell(u)$ and $\ell(v)$ differ by more than one. We generally tolerate concurrencies, but aim to keep their number low. Therefore, to count the number of concurrencies implied with the selected dual graph, we introduce an edge weight $\omega(e)$ for every edge $e \in F_1$. This weight of an edge $e = \{u, v\}$ is set to $\omega(e) = |\ell(u)\Delta\ell(v)| - 1$. Hereby, Δ is the symmetric difference.

Using the node weighting w , the newly introduced edge sets F_1 and F_2 , and the edge weighting ω , we define three objective functions used in our extended problem definition. For a resulting planar graph G' , the kept set elements and set memberships are quantified by f_{weight} . We compute the total number of concurrencies of G' with f_{concur} and count the total number of favorable adjacency relationships between nodes and the outer face by f_{outer} .

Using the additional definitions we extend the problem SetSystemSimplification to MCSetSystemSimplification.

Problem 2 (MCSetSystemSimplification) Given

- a hypergraph $H = (V, E)$,
- the superdual graph $G = (Z, F)$ for H , with $F = F_1 \cup F_2$,
- a node weighting $w: V \rightarrow \mathbb{R}_{>0}$,
- an edge weighting $\omega: F_1 \rightarrow \mathbb{R}_{\geq 0}$, and
- parameters $\alpha, \beta \in \mathbb{R}_{\geq 0}$.

find

- a set $S \subseteq V$ and
- a planar subgraph $G' = (Z', F')$ of the superdual graph G for H ,

such that $G'' = (Z' \setminus \{v_0\}, F_1 \cap F')$ is a planar support of the hypergraph $H - S$ and

$$f(G') = f_{\text{weight}}(G') - \alpha \cdot f_{\text{concur}}(G') + \beta \cdot f_{\text{outer}}(G') \quad (3)$$

is maximized, where

$$f_{\text{weight}}(G') = \sum_{v \in V \setminus S} w(v), \quad (4)$$

$$f_{\text{concur}}(G') = \sum_{e \in F_1 \cap F'} \omega(e), \text{ and} \quad (5)$$

$$f_{\text{outer}}(G') = |F_2 \cap F'|. \quad (6)$$

Here, G'' is the dual graph of the Euler diagram excluding the node v_0 representing the outer face and its incident edges. The hyperedge that corresponds to a set forms a connected component in G'' . This ensures that for each set the corresponding region is connected, which avoids certain violations of the unique curve labels wellformedness condition, such as the one in Fig. 5f. However, we allow regions with holes. Therefore, a solution may contain multiple curves with the same label, i.e., the exterior ring and the multiple interior rings of a region. The function f_{concur} evaluates only the set of edges belonging to G'' , i.e., the set $F_1 \cap F'$. In contrast, the function f_{outer} counts the number of selected edges incident to v_0 , which equals the size of $F_2 \cap F'$.

6. Methodology

In this section we present our exact method and our heuristic for MCSetSystemSimplification; see Sect. 6.1 and Sect. 6.2, respectively. Recall that both methods take the superdual graph $G = (Z, F)$ as input and return a planar subgraph $G' = (Z', F')$ of it, which will serve as the Euler diagram's dual graph.

6.1. An integer linear program

Variables encoding the selected subgraph For each node u of the superdual graph $G = (Z, F)$, we define a binary variable x_u indicating whether the node is part of the selected subgraph G' ($x_u = 1$).

$$x_u \in \{0, 1\} \quad \forall u \in Z \quad (7)$$

Moreover, we introduce one binary variable $z_{u,v}$ for each edge $e = \{u, v\} \in F$. This variable indicates whether e is selected for G' .

$$z_{u,v} \in \{0, 1\} \quad \forall \{u, v\} \in F \quad (8)$$

These z -variables are coupled with the x -variables to ensure that an edge can be selected only if its two incident nodes are selected.

$$z_{u,v} \leq x_u \quad \text{and} \quad z_{u,v} \leq x_v \quad \forall \{u, v\} \in F \quad (9)$$

Objective The x - and z -variables introduced in the previous section are sufficient to express all three objectives of MCSetSystemSimplification.

$$\text{Maximize} \quad \sum_{p \in Z} w(p) \cdot x_p - \alpha \sum_{\{u,v\} \in F_1} \omega(u,v) \cdot z_{u,v} + \beta \sum_{\{v_0,v\} \in F_2} z_{v_0,v} \quad (10)$$

Enforcing connectivity of hyperedges To ensure the connectivity of hyperedges in the selected subgraph G' of G , we adapt a flow model by Shirabe [Shi05] for spatial unit allocation tasks occurring in spatial planning. In our application, we apply the model separately to each hyperedge $X \in E$. For this, we introduce a directed graph $\tilde{G}_X = (Z_X, A_X)$; see Fig. 6. The node set of \tilde{G}_X contains every node of G that is labelled with X , i.e.,

$$Z_X = \{u \in Z \mid X \in \ell(u)\}. \quad (11)$$

The arc set of \tilde{G}_X contains two opposite arcs for each edge of G that connects two nodes labeled with X , i.e.,

$$A_X = \{(u, v), (v, u) \mid \{u, v\} \in F, X \in \ell(u), X \in \ell(v)\}. \quad (12)$$

Due to the definition of G , \tilde{G}_X is a complete, directed graph.

Figure 7 illustrates the flow model that ensures the connectivity of the subset $\{u \in X \mid x_u = 1\}$ selected from X . The flow in \tilde{G}_X is represented with the following variables.

$$y_{u,v}^X \in \{0, \dots, |X| - 1\} \quad \forall X \in E, \forall (u, v) \in A_X \quad (13)$$

These variables are constrained such that only arcs corresponding to edges of G that are selected for G' can carry flow.

$$y_{u,v}^X \leq (|X| - 1) \cdot z_{u,v} \quad \forall (u, v) \in A_X, \forall X \in E \quad (14)$$

Another set of variables models which node acts as a sink of the flow network for X .

$$c_u^X \in \{0, 1\} \quad \forall X \in E, \forall u \in Z_X \quad (15)$$

These variables are constrained such that the network for X can contain at most one sink (node e in Fig. 7, with $c_e^X = 1$).

$$\sum_{u \in Z_X} c_u^X \leq 1 \quad \forall X \in E \quad (16)$$

Finally, the next two constraints ensure that

- every selected node except the sink contributes to at least one unit of flow to the network (i.e., nodes b, c, d in Fig. 7),
- the sink (i.e., node e in Fig. 7) is allowed to receive as much flow as there are nodes in the network, and
- every non-selected node receives no flow (i.e., node a in Fig. 7).

$$\sum_{(v,w) \in A_X} y_{v,w}^X - \sum_{(u,v) \in A_X} y_{u,v}^X \geq x_v - |X| \cdot c_v^X \quad \forall X \in E, \forall v \in Z_X \quad (17)$$

$$\sum_{(u,v) \in A_X} y_{u,v}^X \leq (|X| - 1) \cdot x_v \quad \forall X \in E, \forall v \in Z_X \quad (18)$$

To summarize, every flow that a node contributes to the network for a hyperedge X has to reach the sink and can pass only through nodes selected for X . With this, the model up to now is sufficient to ensure that the nodes selected for hyperedge X induce a connected subgraph in the selected subgraph G' of G .

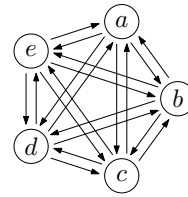


Figure 6: The directed graph \tilde{G}_X for a hyperedge X .

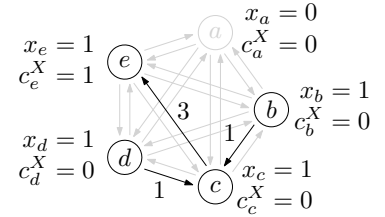


Figure 7: A feasible assignment of the variables modeling the connectivity of the selected subgraph for X .

Enforcing planarity A graph is planar if and only if it does not contain a Kuratowski subdivision as a subgraph (i.e., a subdivision of $K_{3,3}$ or K_5) [Kur30]. Hence, we can ensure the planarity of the output graph G' by requiring that, for each Kuratowski subdivision K contained in G , at least one edge is unselected. For this, we add the constraint

$$\sum_{\{u,v\} \in F(K)} z_{u,v} \leq |F(K)| - 1 \quad \forall K \in \mathcal{K}(G), \quad (19)$$

where $\mathcal{K}(G)$ is the set of all Kuratowski subdivisions contained in G and $F(K)$ is the set of edges of a graph K .

A challenge with this formulation is that there can be exponentially many Kuratowski subdivisions in G . Therefore, setting up the ILP with all the $|\mathcal{K}(G)|$ instances of Constraint 19 is prohibitive in practice. To tackle this challenge, we initially set up the ILP without Constraint 19, but we make sure that the solver detects relevant instances of Constraint 19 during the optimization process and adds them to the model. We implement this idea with a *callback*, which is a customized method that the solver automatically invokes at certain states of the optimization process. The callback that we introduce is invoked whenever the solver finds a new *incumbent solution*, i.e., a solution that satisfies all constraints of the current

model and that is better than any solution found before. For the incumbent solution that led to the invocation of the callback, let G' be the subgraph of G as determined with the z -variables. We apply the Boyer-Myrvold's planarity testing algorithm [BM04] to G' , which either reports that G' is planar or returns a Kuratowski subdivision K of G' , thus proving that G' is non-planar. If G' is planar, we simply resume solving the current model, since there may be better solutions than G' that the solver has not found yet. Else, we instantiate Constraint 19 with the found Kuratowski subdivision K and add this instance of the constraint to the model, before resuming the solution procedure. This strategy is supported by state-of-the-art ILP solvers in a way that guarantees an optimal solution as output.

To strengthen our initial model without Constraint 19, we add the following constraint.

$$\sum_{\{u,v\} \in F} z_{u,v} \leq 3 \cdot \sum_{p \in Z} x_p - 6 \quad (20)$$

This inequality does not ensure planarity but, due to Euler's formula, is valid for all solutions satisfying the planarity requirement.

6.2. Heuristic approach

We now present our heuristic for selecting a planar subgraph $G' = (Z', F')$ of the superdual graph $G = (Z, F)$. The heuristic initializes G' with the node representing the outer face as the only node, i.e., $Z' = \{v_0\}$ and $F' = \emptyset$. Then, it lets G' grow in an iterative and greedy manner, ensuring that after every iteration the connectivity requirement for hyperedges and the planarity requirement are satisfied. With this, the heuristic guarantees a feasible solution to MCSetSystemSimplification, but not an optimal solution.

Algorithm 1 describes the heuristic in more detail. The iterative growth is implemented with a while loop, where in each iteration the method ADDNEXTNODE is called. The method returns true or false, depending on whether it succeeded to grow G' . If the method was unsuccessful, the algorithm terminates and returns G' .

The method ADDNEXTNODE is presented in Algorithm 2. It first computes a list C of candidates, where a candidate c is an extension of G' by one node $c.v \in Z \setminus Z'$ and a set of edges $c.edges$ between $c.v$ and nodes of G' . The candidate list C is obtained as the union of multiple lists, each of which is computed based on one edge $\{p, v\} \in F$ with $p \in Z'$ and $v \in Z \setminus Z'$, using a method CREATEEDGECANDIDATES. This method returns only candidates whose selection satisfies the connectivity requirement (as we will later explain). After C has been set up, we compute for each candidate $c \in C$ the increase in the objective value that its selection would cause and store it as $c.w$. Finally, we go through the candidates in decreasing order of $c.w$ and choose the first candidate that does not violate the planarity requirement. For planarity testing, we use the Boyer-Myrvold algorithm [BM04], as in our ILP-based method.

The method CREATEEDGECANDIDATES yields for a given edge $e = \{p, v\}$ a set of candidates; see Algorithm 3. For every candidate c in this set, $c.v = v$ and $c.edges$ contains e . However, the algorithm returns multiple candidates, which differ with respect to the edges in $c.edges$ in addition to e . To compute this set, let X_1, \dots, X_K be the hyperedges that contain v and whose connectivity would not be achieved when selecting v with edge $e = \{p, v\}$ alone. For example,

Algorithm 1 Heuristic set system simplification

Require: Undirected super dual graph $G = (Z, F)$ with node weights w and edge weights ω

```

1: procedure SIMPLIFY( $G$ )
2:    $Z' \leftarrow \{v_0\}, F' \leftarrow \emptyset, G' \leftarrow (Z', F')$ 
3:    $s \leftarrow \text{True}$ 
4:   while  $s$  do
5:      $s \leftarrow \text{ADDNEXTNODE}(G', G)$ 
   return  $G' = (Z', F')$ 

```

Algorithm 2 Greedy addition of the next node together with edges connecting it to the current graph

Require: Current selected dual graph $G' = (Z', F')$, super dual graph $G = (Z, F)$

```

1: procedure ADDNEXTNODE( $G', G$ )
2:    $\triangleright$  Collect candidates:
3:    $C \leftarrow$  empty list of candidates
4:   for  $(p, v) \in F$  such that  $p \in Z'$  and  $v \notin Z'$  do
5:      $C_{pv} \leftarrow \text{CREATEEDGECANDIDATES}(G', G, p, v)$ 
6:      $C \leftarrow C \cup C_{pv}$ 
7:    $\triangleright$  Rate candidates:
8:   for  $c \in C$  do
9:      $c.w \leftarrow w(c.v) - \alpha \cdot \sum_{e \in c.edges \cap F_1} \omega(e) + \beta \cdot |c.edges \cap F_2|$ 
10:   $\triangleright$  Choose best candidate:
11:  Sort  $C$  descending by weight  $w$ 
12:  while  $C.size > 0$  do
13:     $c \leftarrow C.pollFirst()$ 
14:    Add node  $c.v$  to  $Z'$  and edges  $c.edges$  to  $F'$ 
15:    if isPlanar( $G'$ ) then
16:      return True
17:    else
18:      Remove  $c.v$  from  $Z'$  and  $c.edges$  from  $F'$ 
   return False

```

in Fig. 8, this holds for the hyperedge a . For each such hyperedge, the connectivity can be repaired with a single edge among the edges incident to v other than e , whose number is $\deg(v) - 1$.

Hence, we generate $O((\deg(v) - 1)^K)$ candidates, where $K < |\ell(v)|$. In Fig. 8, this yields two candidates, visualized with different colors. Explicitly enumerating the candidates can be done reason-

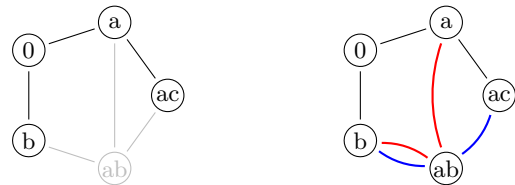


Figure 8: Graph G' (black) after adding three nodes and three edges with our heuristic. Node ab has not been added yet (left). Calling CREATEEDGECANDIDATES for edge $\{a, ab\}$ yields two candidates: The red candidate with edges $\{a, ab\}, \{b, ab\}$ and the blue candidate $\{a, ab\}, \{b, ab\}$ (right).

Algorithm 3 Create candidates for a single edge $\{p, v\}$

```

1: procedure CREATEEDGEcandidates( $G', G, p, v$ )
2:    $C \leftarrow$  empty list of candidates
3:   Let  $\{X_1, \dots, X_K\}$  be the set of hyperedges in  $\ell(v)$  whose
   connectivity would be violated if selecting only  $v$  and  $\{p, v\}$ .
4:   For  $i = 1, \dots, K$  let  $F'_i$  be the set of edges connecting  $v$  with
   a selected node of hyperedge  $X_i$ , i.e., a node in  $X_i$  and  $G'$ .
5:   for  $\epsilon \in F'_1 \times F'_2 \times \dots \times F'_K$  do
6:     Let  $c$  be a new candidate
7:      $c.v = v$ 
8:      $c.edges =$  set containing edge  $\{p, v\}$  and all edges in  $\epsilon$ 
9:      $C.add(c)$ 
return  $C$ 

```

ably fast, assuming that the number $|\ell(v)|$ of hyperedges containing node v is a small constant, which we did in all our experiments with the heuristic. For set systems where $|\ell(v)|$ can be large, one may use our heuristic with a user-set upper limit on the size of $c.edges$.

7. Experiments

Datasets We evaluate our methods with two datasets.

- MovieDB from the 2007 InfoVis contest [KJKC]: Each set system is based on a single director. The sets are the movies of the director. The set elements are actors of the corresponding movie.
- TwitterCircles [LK14]: The dataset consists of users and their interest groups. Each set system is based on a user's ego network. Each set is based on the user's interest circles while the set elements are followed users belonging to at least one interest circle.

In total, there are 930 set systems in TwitterCircles and 16884 in MovieDB. However, we omit all set systems which have less than five nodes in addition to v_0 in the superdual graph as those always have a planar embedding, simply because they cannot have a K_5 or a $K_{3,3}$ as a minor. Thus, we select 281 and 569 set systems, respectively. Table 1 provides further details. For all experiments, we defined the weight of an element as the number of sets containing it, and we applied the optional Step 1, i.e., the condensation of the hypergraph. All experiments were executed on an AMD Ryzen 9 7950X with 64GB of RAM using Java 11 and Gurobi 9.5.1 for solving the ILPs.

The code and datasets are available under a GPL open source license from <https://gitlab.igg.uni-bonn.de/geoinfo/generating-euler-diagrams>.

dataset	#set systems		#sets	#elements
MovieDB	569	Avg	4.39	44.30
		Max	15	288
TwitterCircles	281	Avg	6.19	73.83
		Max	14	197

Table 1: Statistics of MovieDB and TwitterCircles.

Before analyzing the results, we show the full workflow on the set system for the director Keith Hooker from MovieDB in Fig. 9.

This contains 5 sets with 19 set elements. Our ILP approach produces an Euler diagram where each single-labelled face is adjacent to the outer face. Additionally, the minimization of concurrencies results in a nested structure. Nodes with only a few labels are placed near the outer face. In contrast, regions with a higher label count are moved towards the center of the Euler diagram.

Parameter influence To study the influence of the parameters α and β , we computed multiple solutions for all set systems from MovieDB using our ILP approach. For $\beta = 0.1$ and $\alpha = 0.01$ the average number of concurrencies was 1.43 and all set elements were selected. Keeping β fixed and increasing α to 1.25 reduces the average number of concurrencies per Euler diagram by 54.98%, while the weight of the selected set elements decreases by 0.42%.

Our goal is to demonstrate the complexity of the datasets and the advantages of our simplification through a single example. Therefore, the director Joel Schoenbach is shown in Fig. 10. This example shows that our approach can simplify the set system to reduce concurrency. However, this comes at the cost of the removal of elements. We show additional examples in the supplemental material.

Similarly, we investigate the influence of the parameter β . We compute two solutions for the same set system; see Fig. 11. Both solutions were obtained with $\alpha = 0.01$. On the left, we set $\beta = 0.1$. On the right, we set $\beta = 0$, which results in only a single node being adjacent to the outer face. The latter leads to a hardly readable visualization. The sets are nested and form holes within the set that is connected to the outer face. Comparing both Euler diagrams, it is harder to follow individual set outlines for $\beta = 0$. As a result, it would be difficult to determine labels within the interior of the diagram when only a single label for each curve is given.

Comparison of solutions of exact method and heuristic We now compare the results of the ILP and of the heuristic for the 850 set systems given with the two datasets. For this purpose, we evaluate the value of the overall objective function f and the functions f_{weight} , f_{concur} , f_{outer} expressing the three different criteria of MC-SetSystemSimplification. Based on our experiences with the different parameter settings discussed in the previous section, we fixed $\alpha = 0.01$ and $\beta = 0.1$ for all the experiments that we report here.

We used a time limit of one hour for the ILP solver and report the best solution. For all 850 set systems, the solver found a solution within the time limit, but in four examples from TwitterCircles the solver was not able to prove the optimality of the solution. In three cases, the solution contained 100% of the total weight of the set system. In one example (id = 779715) a solution with 50.82% of the total weight was returned and a gap of 96.64% was reported, meaning that there might be a solution whose objective value is roughly twice as high as that of the found solution.

Across all instances, we observe that the heuristic performs worse than the ILP, in the sense that it achieves a lower value for the objective function f (see the column f in Table 2 for MovieDB and Table 3 for TwitterCircles). This is mainly due to two factors: the heuristic includes less node weight in the dual graph (column f_{weight}) and selects edges with more concurrency (column f_{concur}).

For all instances in MovieDB, our ILP approach found a planar

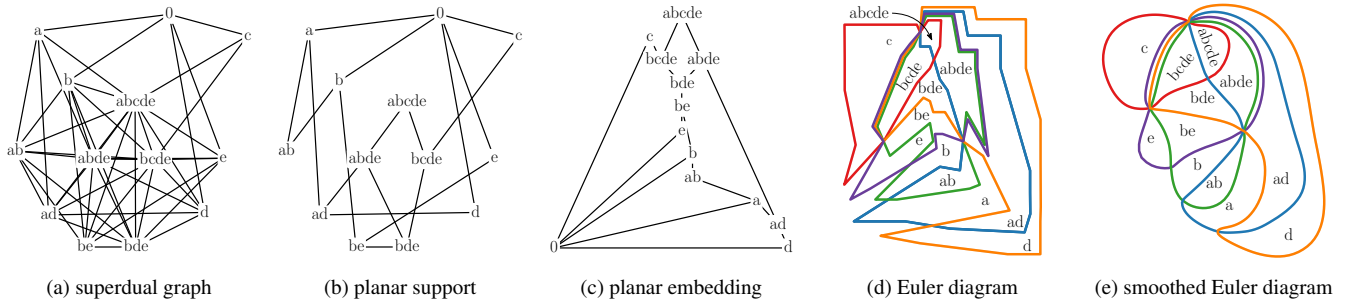


Figure 9: Euler diagram of the set system corresponding to the director Keith Hooker from MovieDB.

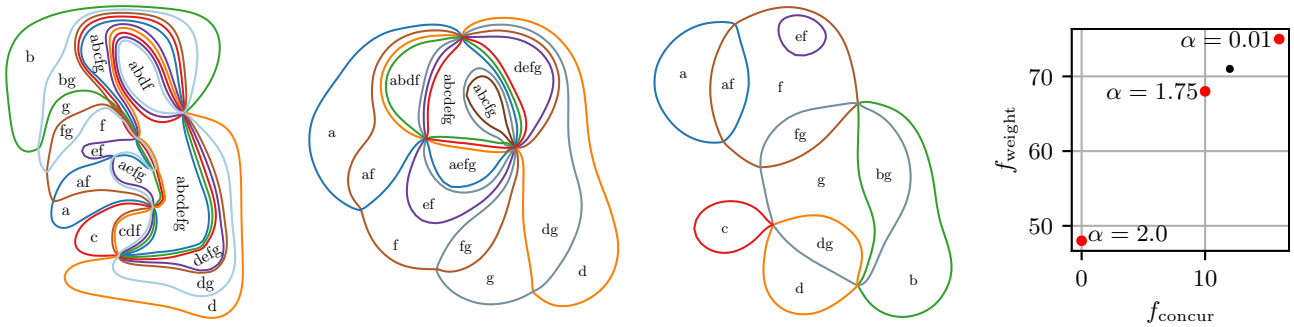


Figure 10: Simplifying the set system of director Joel Schoenbach from left to right. The left figure is computed using $\alpha = 0.01$ with $f_{weight} = 75$ and $f_{concur} = 16$. The middle figure yields $f_{weight} = 68$ and $f_{concur} = 10$ for $\alpha = 1.75$. The lowest concurrency $f_{weight} = 48$ and $f_{concur} = 0$ is a result of $\alpha \geq 2.0$. $\beta = 0.1$ is fixed for all results. The diagram on the right shows the relation between f_{weight} and f_{concur} for the shown example when changing α . The red data points correspond to the visualized Euler diagrams.

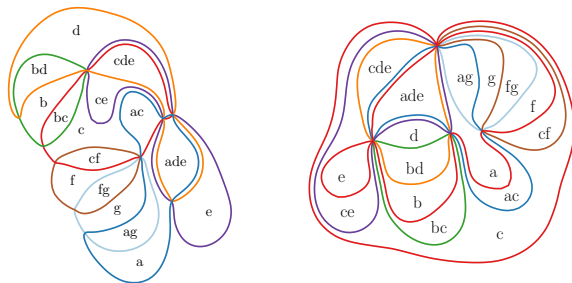


Figure 11: Comparison of results for director Art Camacho for $\beta = 0.1$ (left) and $\beta = 0$ (right); $\alpha = 0.01$ for both. For $\beta = 0$, only one node of the dual graph, i.e. labelled c , is adjacent to the outer face.

support with all set elements. In contrast, the heuristic did not include all set elements in every solution. The average value of f_{weight} is 0.05% less with the heuristic than with the ILP. For the instances in TwitterCircles, the ILP in a single case yielded a solution without all set elements, and the average value of f_{weight} is 0.16% less with the heuristic than with the ILP.

To evaluate the results with respect to concurrent curves, we compare the average values of f_{concur} of our approaches. For TwitterCircles, f_{concur} increased from 2.02 to 4.12. For MovieDB, f_{concur} increased from 1.43 to 2.78. This increased number of

Method		f	f_{weight}	f_{concur}	f_{outer}	Time [s]
ILP	Avg	50.68	50.26	1.43	4.08	0.221
	Max	294.66	294	55	14	99.3485
Heuristic	Avg	50.68	50.26	2.78	4.07	0.0003
	Max	294.66	294	90	14	0.018

Table 2: Results of the ILP and the heuristic on MovieDB. Avg and Max are the average and maximum over all instances.

Method		f	f_{weight}	f_{concur}	f_{outer}	Time [s]
ILP	Avg	128.73	128.20	2.02	5.06	54.05
	Max	1069.16	1069	89	13	3,602.53
Heuristic	Avg	128.50	127.99	4.12	5.00	0.003
	Max	1069.08	1069	111	13	0.267

Table 3: Results of the ILP and the heuristic on TwitterCircles. Avg and Max are the average and maximum over all instances.

concurrent curves is also reflected by the maximum values of f_{concur} , which increased from 89 to 111 and from 55 to 90, respectively.

We investigate the distribution of the increased number of concurrent curves by the factor of two in Fig. 12. None of the instances drastically exceeds this factor. The additional concurrencies are well distributed across all instances in MovieDB. As an example,

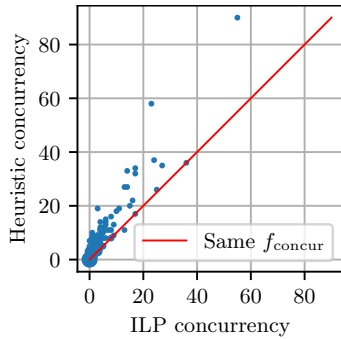


Figure 12: Comparison of concurrency of our heuristic and ILP approach. Each point represents a set system in MovieDB.

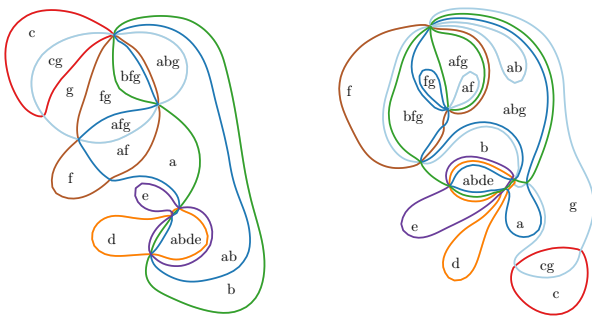


Figure 13: Resulting Euler diagrams for director Brett Ryan Bonowicz using the ILP (left) and the heuristic (right).

the results of both approaches for the director Brett Ryan Bonowicz are shown in Fig. 13. In that case, the additional concurrency is well distributed across the visualization and the maximum number of concurrencies occurring between two adjacent zones is the same for the ILP as for the heuristic.

Comparison of running times We measured the running times of the heuristic and the ILP (see the last columns in Tables 2 and 3). Each running time includes the time for Steps 1–3. It excludes the running time for Steps 4–6, as these steps are not our contribution. The maximum running time of TwitterCircles of roughly one hour is due to the time limit.

We observe a large difference between the ILP and the heuristic for both the average and maximum values. On the other hand, we can compute an optimal dual graph of Euler diagrams for the movie dataset within the time limit using our ILP. However, the heuristic is 138 times faster than the ILP on average. Setting a time limit of 10s for the ILP solver results in the same order of speedup for TwitterCircles. However, such a constrained time limit for the ILP solver leads to worse results than the heuristic.

Comparison with an existing method Finally, we compared our exact method with the method by Rodgers et al. [RZF08], which allows sets to be split into multiple regions, breaking the duplicate curve label wellformedness condition as well as drawing layouts with concurrency, see Section 4.1. This is the closest state-of-the-art to our method. First, using our exact method, we identified all

set systems in MovieDB that do not admit an Euler diagram with connected regions and without concurrency. This yielded 187 set systems. For each of them, we used the method of Rodgers et al. to generate an Euler diagram. In 18.2% of the cases, the resulting Euler diagram splits at least one set into two or more regions. In contrast, in every case, our exact method with $\alpha = 0.01$ and $\beta = 0.1$ yielded an Euler diagram with a single connected region for each set and without losing a set element. Moreover, on average over all 187 set systems, our ILP reduced the concurrency by 35.35%.

8. Conclusion

We have proposed a novel ILP approach for finding a planar support of a given hypergraph that represents a set system. We have integrated this approach into a complete workflow for generating Euler diagrams that represent each set as a single connected region. The ILP maximizes the preserved number of set elements or set memberships. Additionally, it minimizes the total number of concurrent curves and places a maximum number of faces contained in only few curves adjacent to the outer face. Moreover, we have developed a heuristic that tries to optimize the same objective by greedily adding nodes to an empty graph. Our experiments show that our ILP can be used to produce optimal general Euler diagrams which comply with our wellformedness criteria. Moreover, our approach can simplify a set system in order to reduce concurrency. Comparisons of the heuristic with the ILP show that the heuristic produces results with similar objective values while increasing the concurrency by a factor of two. A benefit of the heuristic is that it needs only a fraction of the processing time.

For future work, producing Euler diagrams without concurrency by either limiting the edges within the superdual graph or merging sets might be possible. When concurrency can not be avoided, equally distributing concurrency across edges instead of accumulating the total concurrency in a single edge is favorable. To improve readability, we could consider additional well-formedness conditions, such as the avoidance of triple points. With regards to the heuristic, the computation of candidates can be improved to avoid the brute force approach. For doing this, the algorithm needs to update existing candidates when new nodes are added to the dual graph. Additionally, it might be beneficial to exclude certain edges from candidate creation [WMT23]. Our ILP could be accelerated, e.g., by generating multiple Kuratowski subdivisions at once [CHW19], instead of one by one. It would also be possible to explore ways of displaying removed set elements and indicating the lost information using visual mechanisms, such as texture, shading or icons. Furthermore, it would be interesting to encode the degree of simplification and completeness of the Euler diagram using visualizations for quantitative information, such as area proportional layouts [SRH11] or applying a color scale [SGS*18].

Acknowledgements. For the purpose of open access, the author has applied a Creative Commons Attribution (CC-BY) license to any Author Accepted Manuscript version arising from this submission. We thank Dagstuhl Seminar 22462 “Set Visualization and Uncertainty” (November 13-18, 2022) for initializing this research. BW was partially supported by grants DOE DE-SC0021015 and NSF IIS-2145499.

References

- [AMA*16] ALSALLAKH B., MICALLEF L., AIGNER W., HAUSER H., MIKSCH S., RODGERS P. J.: The state-of-the-art of set visualization. *Computer Graphics Forum* 35, 1 (2016), 234–260. doi:10.1111/cgf.12722. 3
- [ARRC11] ALPER B., RICHE N., RAMOS G., CZERWINSKI M.: Design study of linesets, a novel set visualization technique. *IEEE Trans. on Visualization and Computer Graphics* 17, 12 (2011), 2259–2267. doi:10.1109/TVCG.2011.186. 4
- [BCPS11] BRANDES U., CORNELSEN S., PAMPEL B., SALLABERRY A.: Blocks of hypergraphs. In *Combinatorial Algorithms* (2011), pp. 201–211. doi:10.1007/978-3-642-19222-7_21. 4
- [BKM*11] BUCHIN K., KREVELD, VAN M., MEIJER H., SPECKMANN B., VERBEEK K.: On planar supports for hypergraphs. *Journal of Graph Algorithms and Applications* 15, 4 (2011), 533–549. doi:10.7155/jgaa.00237. 4
- [BM04] BOYER J. M., MYRVOLD W. J.: On the cutting edge: Simplified $O(n)$ planarity by edge addition. *Journal of Graph Algorithms and Applications* 8, 3 (2004), 241–273. doi:10.7155/jgaa.00091. 7
- [Bra12] BRATH R.: Multi-attribute glyphs on Venn and Euler diagrams to represent data and aid visual decoding. In *Proc. 3rd Int. Workshop on Euler Diagrams* (2012), vol. 854 of *CEUR*, pp. 122–129. 3
- [CHW19] CHIMANI M., HEDTKE I., WIEDERA T.: Exact algorithms for the maximum planar subgraph problem: New models and experiments. *ACM J. Exp. Algorithmics* 24 (2019). doi:10.1145/3320344. 5, 10
- [CP95] CHROBAK M., PAYNE T.: A linear-time algorithm for drawing a planar graph on a grid. *Information Processing Letters* 54, 4 (1995), 241–246. doi:10.1016/0020-0190(95)00020-D. 2
- [CR05] CHOW S., RUSKEY F.: Towards a general solution to drawing area-proportional Euler diagrams. *Electronic Notes in Theoretical Computer Science* 134 (2005), 3–18. doi:10.1016/j.entcs.2005.02.017. 4
- [DvKSW12] DINKLA K., VAN KREVELD M., SPECKMANN B., WESTENBERG M. A.: Kelp diagrams: Point set membership visualization. *Computer Graphics Forum* 31, 3 (2012), 875–884. doi:10.1111/j.1467-8659.2012.03080.x. 4
- [EHKP15] EFRAT A., HU Y., KOBOUROV S. G., PUPYREV S.: MapSets: Visualizing embedded and clustered graphs. *J. Graph Algorithms and Applications* 19, 2 (2015), 571–593. doi:10.7155/jgaa.00364. 4
- [FH02] FLOWER J., HOWSE J.: Generating Euler diagrams. In *Diagrammatic Representation and Inference* (2002), pp. 61–75. doi:10.1007/3-540-46037-3_6. 3
- [GCH*21] GEIGER J., CORNELSEN S., HAUNERT J.-H., KINDERMANN P., MCHEDLIDZE T., NÖLLENBURG M., OKAMOTO Y., WOLFF A.: ClusterSets: Optimizing planar clusters in categorical point data. *Computer Graphics Forum* 40, 3 (2021), 471–481. doi:10.1111/cgf.14322. 4
- [GHK09] GANSNER E. R., HU Y., KOBOUROV S. G.: GMap: Drawing graphs as maps. In *Proc. Graph Drawing (GD'09)* (2009), vol. 5849 of *LNCSE*, pp. 405–407. doi:10.1007/978-3-642-11805-0_38. 4
- [JP87] JOHNSON D. S., POLLAK H. O.: Hypergraph planarity and the complexity of drawing Venn diagrams. *J. Graph Theory* 11, 3 (1987), 309–325. doi:10.1002/jgt.3190110306. 2, 4
- [KGWD22] KEHLBECK R., GÖRTLER J., WANG Y., DEUSSEN O.: SPEULER: Semantics-preserving Euler Diagrams. *IEEE Trans. on Visualization and Computer Graphics* 28, 1 (2022), 433–442. doi:10.1109/TVCG.2021.3114834. 3
- [KJKC] KOSARA R., JANKUN-KELLY T. J., CHLAN E.: IEEE InfoVis 2007 contest: InfoVis goes to the movies. <https://eagereyes.org/blog/2007/infovis-contest-2007-data>. 8
- [KMN14] KLEMZ B., MCHEDLIDZE T., NÖLLENBURG M.: Minimum tree supports for hypergraphs and low-concurrency Euler diagrams. In *Algorithm Theory - SWAT 2014* (2014), vol. 8503 of *LNCSE*, pp. 265–276. doi:10.1007/978-3-319-08404-6_23. 4
- [KS03] KORACH E., STERN M.: The clustering matroid and the optimal clustering tree. *Mathematical Programming* 98, 1-3 (2003), 385–414. doi:10.1007/S10107-003-0410-X. 4
- [Kur30] KURATOWSKI C.: Sur le probleme des courbes gauches en topologie. *Fundamenta mathematicae* 15, 1 (1930), 271–283. 6
- [KvKS09] KAUFMANN M., VAN KREVELD M., SPECKMANN B.: Subdivision drawings of hypergraphs. In *Proc. Graph Drawing* (2009), vol. 5417 of *LNCSE*, pp. 396–407. doi:10.1007/978-3-642-00219-9_39. 4
- [LGS*14] LEX A., GEHLENBORG N., STROBELT H., VUILLEMOT R., PFISTER H.: Upset: visualization of intersecting sets. *IEEE Trans. Visualization and Computer Graphics* 20, 12 (2014), 1983–1992. doi:10.1109/TVCG.2014.2346248. 4
- [LK14] LESKOVEC J., KREVL A.: SNAP Datasets: Stanford large network dataset collection. <http://snap.stanford.edu/data>, 2014. 8
- [Mäk90] MÄKINEN E.: How to draw a hypergraph. *Int. J. Comput. Math.* 34, 3-4 (1990), 177–185. doi:10.1080/00207169008803875. 4
- [MRS*13] MEULEMANS W., RICHE N. H., SPECKMANN B., ALPER B., DWYER T.: KelpFusion: A hybrid set visualization technique. *IEEE Trans. on Visualization and Computer Graphics* 19, 11 (2013), 1846–1858. doi:10.1109/TVCG.2013.76. 4
- [NW88] NEMHAUSER G. L., WOLSEY L. A.: *Integer and Combinatorial Optimization*. Wiley interscience series in discrete mathematics and optimization. 1988. doi:10.1002/9781118627372. 4
- [OZZ23] OLIVER P., ZHANG E., ZHANG Y.: Scalable hypergraph visualization. *IEEE Trans. on Visualization and Computer Graphics* (2023), 1–11. doi:10.1109/TVCG.2023.3326599. 4
- [PKS*23] PAETZOLD P., KEHLBECK R., STROBELT H., XUE Y., STORANDT S., DEUSSEN O.: Recteuler: Visualizing intersecting sets using rectangles. *Computer Graphics Forum* 42, 3 (2023), 87–98. doi:10.1111/cgf.14814. 3
- [RR18] RAMAN R., RAY S.: Planar Support for Non-piercing Regions and Applications. In *Proc. 26th Annual European Symposium on Algorithms (ESA 2018)* (2018), vol. 112 of *LIPICs*, pp. 69:1–69:14. doi:10.4230/LIPICs.ESA.2018.69. 4
- [RWB*23] ROTTMANN P., WALLINGER M., BONERATH A., GEDICKE S., NÖLLENBURG M., HAUNERT J.-H.: MosaicSets: Embedding set systems into grid graphs. *IEEE Trans. on Visualization and Computer Graphics* 29, 1 (2023), 875–885. doi:10.1109/TVCG.2022.3209485. 4
- [RZF08] RODGERS P., ZHANG L., FISH A.: General euler diagram generation. In *Diagrammatic Representation and Inference* (2008), pp. 13–27. doi:10.1007/978-3-540-87730-1_6. 1, 2, 3, 5, 10
- [RZP11] RODGERS P., ZHANG L., PURCHASE H.: Wellformedness properties in Euler diagrams: Which should be used? *IEEE Trans. on Visualization and Computer Graphics* 18, 7 (2011), 1089–1100. doi:10.1109/TVCG.2011.143. 2, 3, 5
- [SA08] SIMONETTO P., AUBER D.: Visualise Undrawable Euler Diagrams. In *12th Int. Conference Information Visualisation* (2008), pp. 594–599. doi:10.1109/IV.2008.78. 1, 3
- [SAA09] SIMONETTO P., AUBER D., ARCHAMBAULT D.: Fully automatic visualisation of overlapping sets. *Computer Graphic Forum* 28, 3 (2009), 967–974. doi:10.1111/j.1467-8659.2009.01452.x. 3
- [SAAB11] SIMONETTO P., ARCHAMBAULT D., AUBER D., BOURQUI R.: ImPrEd: An improved force-directed algorithm that prevents nodes from crossing edges. *Computer Graphics Forum* 30, 3 (2011), 1071–1080. doi:10.1111/j.1467-8659.2011.01956.x. 3

- [SAS16] SIMONETTO P., ARCHAMBAULT D., SCHEIDEGGER C.: A Simple Approach for Boundary Improvement of Euler Diagrams. *IEEE Trans. on Visualization and Computer Graphics* 22, 1 (2016), 678–687. doi:10.1109/TVCG.2015.2467992. 2, 3, 5
- [SGS*18] SCHLOSS K. B., GRAMAZIO C. C., SILVERMAN A. T., PARKER M. L., WANG A. S.: Mapping color to meaning in colormap data visualizations. *IEEE Trans. on Visualization and Computer Graphics* 25, 1 (2018), 810–819. doi:10.1109/TVCG.2018.2865147. 10
- [Shi05] SHIRABE T.: A model of contiguity for spatial unit allocation. *Geographical Analysis* 37, 1 (2005), 2–16. doi:10.1111/j.1538-4632.2005.00605.x. 4, 6
- [SRH11] STAPLETON G., RODGERS P., HOWSE J.: A general method for drawing area-proportional Euler diagrams. *Journal of Visual Languages & Computing* 22, 6 (2011), 426–442. doi:10.1016/j.jvlc.2011.07.001. 10
- [SRHT07] STAPLETON G., RODGERS P., HOWSE J., TAYLOR J.: Properties of Euler diagrams. *Electronic Communications of the EASST* 7 (2007). doi:10.14279/tuj.eceasst.7.92. 3
- [TvGW*19] THOM C., VAN GARDEREN M., WOUTER M., MARTIN N., XIAORU Y.: Short plane supports for spatial hypergraphs. *Journal of Graph Algorithms and Applications* 23, 3 (2019), 463–498. doi:10.7155/jgaa.00499. 4
- [vBKK*22] VAN BEVERN R., KANJ I. A., KOMUSIEWICZ C., NIEDERMEIER R., SORGE M.: The role of twins in computing planar supports of hypergraphs, 2022. arXiv:1511.09389. 2, 4
- [VV04] VERROUST A., VIAUD M.: Ensuring the Drawability of Extended Euler Diagrams for up to 8 Sets. In *Diagrammatic Representation and Inference* (2004), vol. 2980 of LNCS, pp. 128–141. doi:10.1007/978-3-540-25931-2_13. 4
- [WMT23] WAGENINGEN S. V., MCHEDLIDZE T., TELEA A.: Identifying Cluttering Edges in Near-Planar Graphs. In *EuroVis 2023 - Short Papers* (2023), The Eurographics Association. doi:10.2312/evs.20231048. 10
- [ZRPW23] ZHOU Y., RATHORE A., PURVINE E., WANG B.: Topological simplifications of hypergraphs. *IEEE Trans. on Visualization and Computer Graphics* 29, 7 (2023), 3209–3225. doi:10.1109/TVCG.2022.3153895. 4